The Dynamics Beamline at SSRF

Zhen Liu [1], Lihua Wang [1,*], Yong Jiang [1], Yajun Tong [2], Huachun Zhu [1], Te Ji [1], Min Chen [1], Zheng Jiang [1], Xiangjun Wei [1,*]

[1]Shanghai Advanced Research Institute, Chinese Academy of Sciences, Shanghai 201204, China

[2]ShanghaiTech University, Shanghai, 201210, China

*Corresponding author. E-mail: lhwang@sari.ac.cn

*Corresponding author. E-mail: weixj@sari.ac.cn

Abstract: The Dynamics beamline (D-Line), which combines synchrotron radiation infrared spectroscopy (SR-IR) and energy-dispersive X-ray absorption spectroscopy (ED-XAS), is the first beamline in the world to realize concurrent ED-XAS and SR-IR measurements at the same sample position on a millisecond time-resolved scale. This combined technique is effective for investigating rapid structural changes in atoms, electrons, and molecules in complicated disorder systems, such as those used in physics, chemistry, materials science, and extreme conditions. Moreover, ED-XAS and SR-IR can be used independently in the two branches of the D-Line. The ED-XAS branch is the first ED-XAS beamline in China, which uses a tapered undulator light source and can achieve approximately 2.5 × 10^{12} photons/s•300 eV BW@7.2 keV at the sample position. An exchangeable polychromator operating in the Bragg-reflection or Laue-transmission configuration is used in different energy ranges to satisfy the requirements for beam size and energy resolution. The focused beam size is approximately 3.5 μm (H) × 21.5 μm (V), and the X-ray energy range is 5–25 keV. Using one- and two-dimensional position-sensitive detectors with frame rates of up to 400 kHz enables time resolutions of tens of microseconds to be realized. Several distinctive techniques, such as the concurrent measurement of in-situ ED-XAS and infrared spectroscopy, time-resolved ED-XAS, high-pressure ED-XAS, XMCD, and pump–probe ED-XAS, can be applied to achieve different scientific goals.

Keywords: ED-XAS, SR-IR, Time-Resolved, D-Line, SSRF

1. Introduction

The Shanghai Synchrotron Radiation Facility (SSRF) is a third-generation synchrotron radiation light source with a storage ring energy of 3.5 GeV and a circumference of 432 m. User operation commenced at the SSRF on May 6, 2009, with seven Phase-I beamlines fully available to users [1-3]. The SSRF Phase-I Project includes only the X-ray absorption fine structure (XAFS) beamline BL14W1, which is based on a double-crystal monochromator (DCM) [4]. To enable rapid investigations into the complicated atomic and molecular structures in non-equilibrium dynamic processes,

the Dynamics beamline (D-Line) was constructed at the SSRF. It is one of the new beamlines in the SSRF Phase-II Beamline Project and has enabled simultaneous time-resolved measurements of synchrotron radiation infrared spectroscopy (SR-IR) and energy-dispersive X-ray absorption spectroscopy (ED-XAS) at the same sample position. Using this combined technique, time-resolved dynamic correlation information of local atomic, electronic, and molecular structures in complicated systems can be obtained simultaneously, which is critical for accurately understanding the relationship between material structure and function, as well as complex physical and chemical phenomena. Furthermore, it facilitates investigations into the structure–activity relationship of catalytic reaction processes, the structural transformation of matter, molecular and nanostructure assembly processes, and the surface-interface reaction kinetics of materials.

Non-equilibrium states exist universally in the fields of physics, chemistry, and life sciences. In general, non-equilibrium states or transient states are typically accompanied by order-disorder transitions, complex phase behaviors, and the rapid evolution of atomic and molecular structures. These intermediate structures and their interactions determine the reaction direction and final products. Reaction kinetics is investigated to understand the evolution of non-equilibrium states and their underlying mechanisms, thus allowing the reaction products to be predicted or regulated [5,6]. To reveal the dynamic behaviors of such complex systems, the analysis performed should exhibit certain properties: 1) high time resolution to monitor the reaction processes, and 2) simultaneous and multiple probes to obtain complementary information regarding dynamic structures [7,8].

X-ray absorption spectroscopy (XAS) and infrared (IR) spectroscopy are complementary techniques for investigating dynamic processes [9-11]. XAS is a unique synchrotron technique used to investigate the local atomic structure in ordered and disordered systems to identify subtle structural distortions or to characterize partial and local electronic properties, whereas IR spectroscopy reveals molecular structures by exploiting the fact that molecules absorb specific frequencies. In ED-XAS, X-ray energies with a certain bandwidth and energy resolution required for XAS

measurements are dispersed and focused by a bending crystal, and the spectra are recorded by a rapid position-sensitive detector (PSD) for all X-ray energies simultaneously after absorbed by the samples [12,13]. The positions of the beam incident on the detector can be directly correlated with the energy. The main advantages of ED-XAS over the typical energy-scanning XAS are the short acquisition time due to the parallel acquisition of the entire spectrum, a beam spot of several micrometers due to the natural strong focusing features, and high stability during measurement due to the absence of mechanical movement. ED-XAS data can be obtained within microseconds using a rapid PSD [14-16]. In SR-IR, a time resolution of tens of milliseconds can be achieved using the rapid scan mode of FTIR. Therefore, using ED-XAS combined with IR spectroscopy, complementary structural information can be obtained, thus facilitating understanding regarding complex physical and chemical phenomena. Many scientific fields, such as catalysis, condensed matter physics, high-pressure physics, and nanomaterials, will benefit from this technique.

Many ED-XAS beamlines exist in major synchrotron radiation facilities worldwide. The French LURE was the earliest light source used to perform ED-XAS measurements [17-19]. Subsequently, the ODE beamline, which is the dedicated energy-dispersive XAS beamline at the SOLEIL synchrotron light source, was constructed to conduct matter structure studies pertaining to time-resolved, magnetic circle dichroism and structures under extreme conditions [20,21]. ID24 at the European Synchrotron Radiation Facility (ESRF), which is the first ED-XAS beamline in the world that uses a series of insert devices, can achieve a few microns focused beamsize and ~10^{14} photon flux at the sample position. It is the first beamline in the world that enables investigations into catalysis structures via ED-XAS and FT-IR (based on the internal source) combined [22,23]. Time-resolved structures of catalysts have been investigated at several energy-dispersive XAFS beamlines, such as the NW2A and BL-9C, at the Photon Factory in Japan [24-26]. The ED-XAS beamlines based on an inserted device source have also been constructed at Spring-8 in Japan and the Diamond in the UK [27-29].

The D-Line at the SSRF is the first beamline in the world to perform in-situ detections of atomic, electronic, and molecular structures of complex systems using the

SR-IR and ED-XAS combined. The ED-XAS branch is the first energy-dispersive XAFS beamline in China. Considering national strategic requirements, scientific requirements, and methodological characteristics, the D-Line is constructed to investigate the following:

- The relationships between a dynamic structure and its activity in catalytic reactions: Dynamic in-situ monitoring of a catalyst and its process is conducted to understand the catalytic mechanism at the atomic and molecular levels, achieve reaction-direction selection and control, and regulate the reaction products [30-33].
- Phase transitions of condensed matter: The structures and phase-transition mechanisms of various substances, high-temperature superconductors, transition metal oxides, and magnetic materials are investigated under extreme conditions [34-36].
- Assembly process of molecules and nanostructures: The electron transfer, energy transfer, and chemical conversion during the evolution of self-assembled structures are investigated [37,38].
- Surface and interface kinetics of materials: The molecular adsorption process, surface and interface formation, as well as the structure and properties of materials are investigated [39-41].

2. Beamline

2.1 Light source

The source of the ED-XAS branch (BL05U) of the D-Line is an in-vacuum undulator (IVU) with 98 periods and a period length of 22 mm. The maximum peak magnetic field is 0.9 T. The IVU light source provides a significantly amount of flux photons for rapid time resolution. The energy of the ED-XAS branch ranged from 5 to 25 keV, which encompassed the absorption edges from the Ti K-edge to the Ag K-edge. The required energy bandwidth for XAFS is achieved by tapering the magnetic field of the undulator.

The IR light of the IR branch (BL06B) is extracted from both bending magnet radiation and edge radiation in the storage ring. The extraction solid angles in the horizontal and vertical directions are 40 mrad (-15 to +25 mrad) and 20 mrad (-10 to +10 mrad), respectively. The brightness is two to three orders of magnitude higher than

that of a blackbody, from near IR to far IR.

2.2 Beamline layout

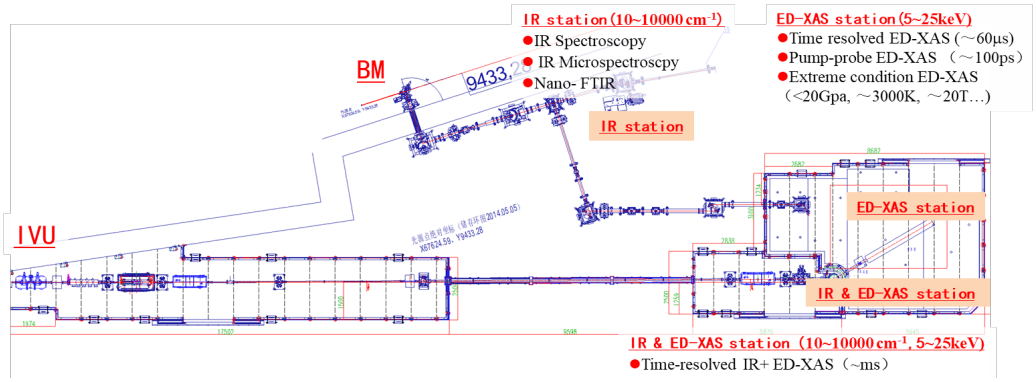

Fig. 1 Layout of D-Line and its three endstations.

The layout of the D-Line and its three endstations are shown in Fig. 1. The optics of the ED-XAS branch are shown schematically in Fig. 2. Meanwhile, the main optics parameters and their functions are listed in Table 1.

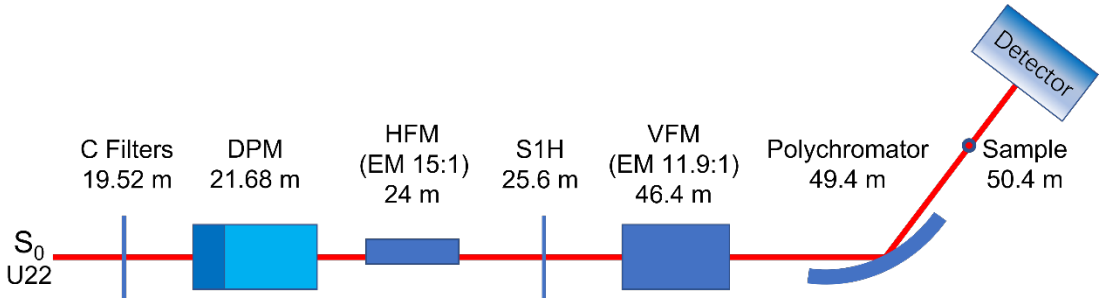

Fig. 2 Layout of ED-XAS branch.

Table 1. Main optics of ED-XAS branch

Main optics	Distance to source (m)	Specifications	Function
Source	0	IVU(tapered): 22 mm period length, 98 periods, 0.9 T magnetic field	Provide high flux density X-ray for time-resolved XAFS
filter	19.5	Material: CVD diamond Thickness:0.03~1.2 mm	Absorb the low energy power
DPM	21.7	Shape: plane Coating layers: Si, Rh and Pt Incident angle:2.5~5 mrad	Cutoff the high energy heat load and reject the high harmonics
HFM	24	Shape: elliptical Coating layers: Rh and Pt Incident angle: 3 mrad	Focus the horizontal beam size and enlarge the horizont-all divergence up to

			1.2 mrad
VFM	46.4	Shape: elliptical Coating layers: Rh and Pt Incident angle: 3mrad	Focus the vertical beam size
Polychromator	49.4	Bragg: Si(111), Si(311), 5~15 keV, elliptical Laue: Si(311), 5~25 keV, cylindrical	Energy dispersive and focus

To reduce the heat load at the polychromator, a set of C-filters (CVD diamond) is used to absorb undesired low-energy power, whereas a double plane mirror (DPM) is used to cut off undesired high-energy power and reject high harmonics. Using this optical configuration, the power density of the polychromator is reduced to approximately 1 W/mm^2. The filters are classified into four groups, with each composed of three exchangeable filters with different thicknesses. The four groups of filters can be selected to achieve a thickness of 0.03–2.4 mm via different combinations. The DPM, which is placed horizontally, is operable in different incident angles (2.5–5 mrad) using three different coating layers (Si, Rh, and Pt).

A horizontal focusing mirror (HFM) with an elliptical shape is used to enlarge the beam horizontal divergence to approximately 1.2 mrad to provide a large footprint on the bending crystal and thus satisfy the demands of bandwidth for XAFS measurements.

The vertical focusing mirror (VFM), which similarly featured an elliptical shape, is used to focus the vertical beam to the sample position. Subsequently, the entire beam can be accepted by one-dimensional (1D) or two- dimensional (2D) PSDs.

The effect of penetration depth at high energies deteriorates both the energy resolution and focal-spot shape; therefore, a polychromator with Bragg and Laue geometries was designed to disperse different X-ray ranges [42]. The Bragg geometry, which uses elliptical a bent Si(111) or Si(311) crystal, operates at 5–15 keV in the reflection mode and delivers a small spot size of 5 μm FWHM in the horizontal direction. The Laue geometry, which uses a bent Si(311) crystal, operates at 15–25 keV in the transmission mode and delivers a large beam measuring dozens to hundreds of micrometers in the horizontal direction. Either one of the two geometries is used depending on the X-ray energy requirements.

Table 2 lists the specifications of the ED-XAS branch of the D-Line measured during the commissioning phase. The focus beam size in the horizontal direction at the sample position reaches 3.5 μm FWHM @Cu K-edge in the Bragg geometry, as shown in Fig. 3. This energy resolution is comparable to that obtained by scanning the DCM at BL11B in the SSRF, as shown in Fig. 4. The flux is approximately 2.5×10^{12} @ Fe K-edge with a bandwidth of 300 eV. The quality of the single Cu XANES remained favorable at an acquisition frequency of 40 kHz, as shown in Fig. 5.

Table 2. Specifications of BL05U beamline

Electron energy (GeV)	3.5
Nature Emittance (nm.rad)	4.22
Light source	IVU (22mm period length and 98 periods)
Energy range (keV)	5-15, Bragg geometry 15-25, Laue geometry
Energy resolution (ΔE/E)	⩽ 1.5×10^{-4} @ Cu K-edge
Beamsize (FWHM)	3.52 μm × 21.59 μm
Flux at sample	2.52×10^{12} phs/s•300 eV BW@7.2 keV
Time resolution	25 μs @Cu K-edge XANES

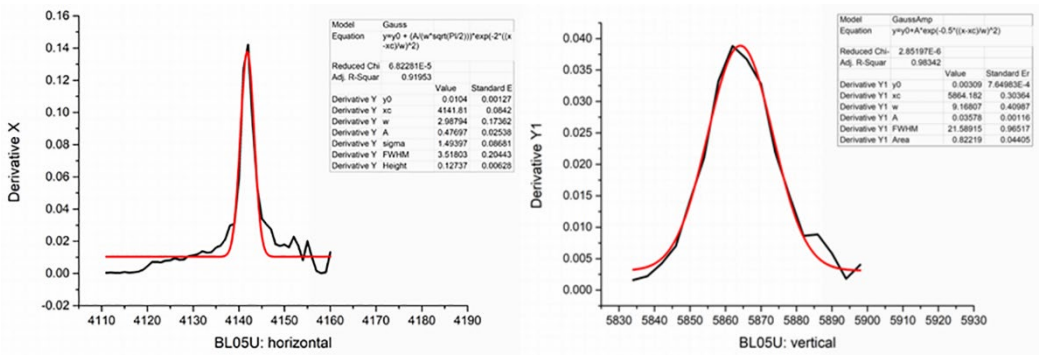

Fig. 3 Gaussian fit (red line) to derivative of knife-edge scan (black line) on sample position along horizontal (right) and vertical (left) directions.

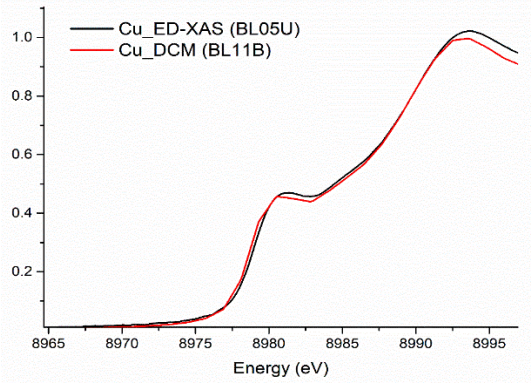

Fig. 4 XANES spectrum of Cu foil obtained via ED-XAS at BL05U (black line) and DCM at BL11B (red line).

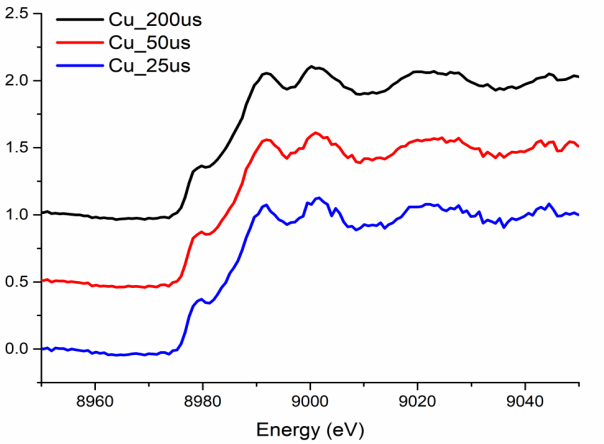

Fig. 5 Cu K-edge XANES acquired at 40 kHz frequency using Gotthard detector.

In the tapered mode, the width of certain harmonics radiated from the undulator is extended sufficiently and the bending crystal at a small radius can disperse X-ray energy with an adequate bandwidth; thus, EXAFS spectra can be obtained at the D-Line. Fig. 6 shows the EXAFS spectra of Ni, Cu, Mo, and Ag acquired from the ED-XAS branch.

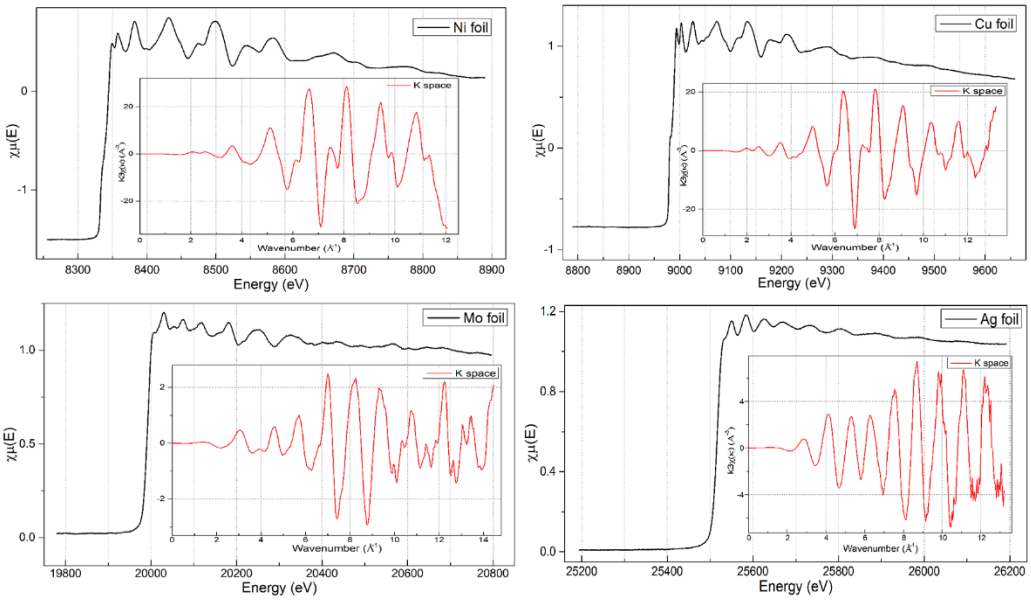

Fig. 6 EXAFS spectra of Ni, Cu, Mo, and Ag acquired at ED-XAS branch.

Fig. 7 is layout of IR branch. Flat mirror M1 is placed 1.806 m below the light source point to extract the IR beam. The IR beam is deflected horizontally by M1 by 90° and enter plane mirror M2 through the radiation protection wall. M2 and M1 are placed 2.209 m apart. Subsequently, the IR beam is deflected from the horizontal direction to

the vertical direction by 90°; it is incident on toroidal mirror T1 and incident on the CVD diamond window after convergent reflection by T1. The distance between T1 and M2 is 0.55 m. The main function of the diamond window is to isolate the ultrahigh vacuum and high vacuum between the beam line and experimental station. To avoid ripples caused by multiple reflections of the window material, the diamond window was machined into a 0.5° wedge structure, and the IR beam level deviated by 0.69°.

The IR beam enter toroidal mirror T2 after passing through the CVD window. The parameters of T2 were designed similarly as those of T1 to obtain minimal aberration. Plane mirror M4 is used for beam steering, i.e., it reflects the beam to the ED-XAS station for coupling. When M4 is inserted into the optical path, the IR beam is reflected to plane mirror M5b and pass through a pair of toroidal mirrors, T3b and T4b, which featured separate meridional and sagittal foci. Subsequently, it is shaped into square spots, transmitted to M7b in the matching system of the joint line station, and then reflected on collimator T5b of the matching system. The collimated beam is reflected by plane mirror M8b and then incident on the joint experimental station. When M4 is removed, the IR beam is incident on the IR-independent experimental station.

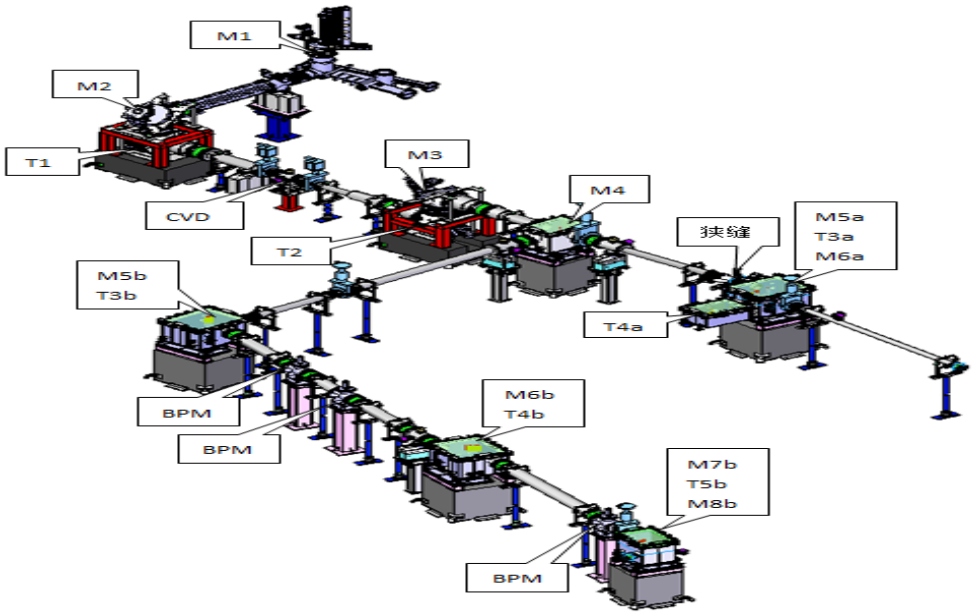

Fig. 7 Layout of IR branch.

3. Experimental station

3.1 2θ ED-XAS optical bench

The ED-XAS setup was installed on a granite table that included the entire surface

of the hutch, which provided high rigidity and stability for equipment installation. The 2θ arm with airpad underneath, which is drive by one motor, can propagate smoothly around the center of the polychromator on the granite table, as shown in Fig. 8. The arm is approximately 3.5 m long and its rotation center is at the center of the polychromator. The four-dimensional sample stage and three-dimensional detector support, with 5 μm resolution and a load capacity of 100 kg, were mounted on the arm to adjust the sample position and detector position. The two stages can propagate along the 2θ arm by the motor with a resolution of 25 μm. Fig. 9 shows a photograph of the ED-XAS station.

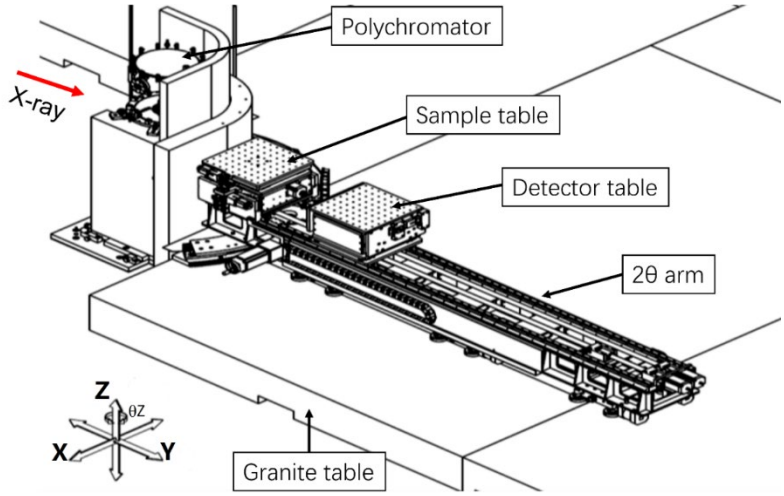

Fig. 8 Schematic illustration of experimental hutch.

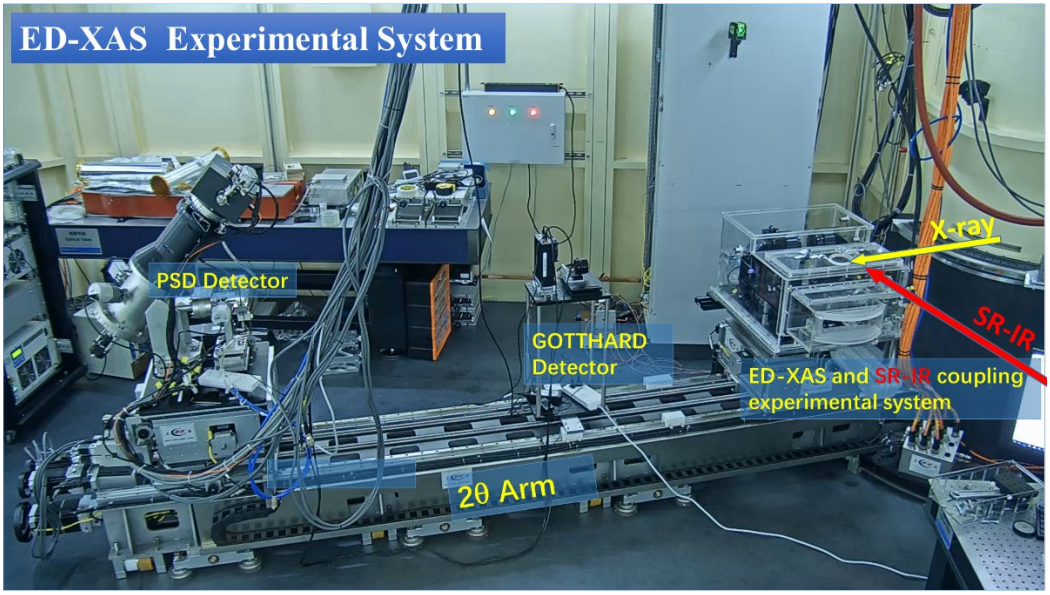

Fig. 9 Photograph of ED-XAS station.

For ED-XAS measurements, the dispersed beam after the polychromator is detected using the 1D or 2D PSD installed at the end of the 2θ arm to maintain the required

energy resolution and total energy range. Table 3 lists the ED-XAS detectors in the D-Line.

Table 3. ED-XAS detectors in D-Line

Type of the detectors	1D（Si）	1D (CCD)	2D（CCD）
Model	Gotthard II	1D PSD	FReLoN 2D
Energy range	5-25 keV	5-25 keV	5-25 keV
Pixel size	50 μm	14 μm	14 μm×14 μm
Pixel number	2048	2048	2048×2048
Frame rate	400kHz (@continuous mode) 4.5MHz (@bursts mode)	4000 frames/s	~1000 frames/s

Gotthard II is a 1D detector system based on the principle of charge integration with automatic gain-switching capability. The detector module is composed of 10 readout application-specific integrated circuit wires bonded to a single silicon sensor with a 4 mm × 8 mm sensitive area that contained 1280 channels at a 50 μm pitch. This detector is characterized by a high frame rate (400 kHz in the continuous mode and up to 4.5 MHz in the burst mode), low noise, and spectral-information availability.

The FReLoN 2D camera used in this study features a horizontal field-of-view of 101 mm, a pixel size of 50 μm, and 2048 × 2048 pixels, which ensure the required energy resolution and total energy range. This detector is characterized by a short readout time of approximately 1 kHz, a high dynamic range, linearity, and spatial (or, equivalently, energy) resolution. Fig. 10 shows the performance yielded by the detector at the D-Line.

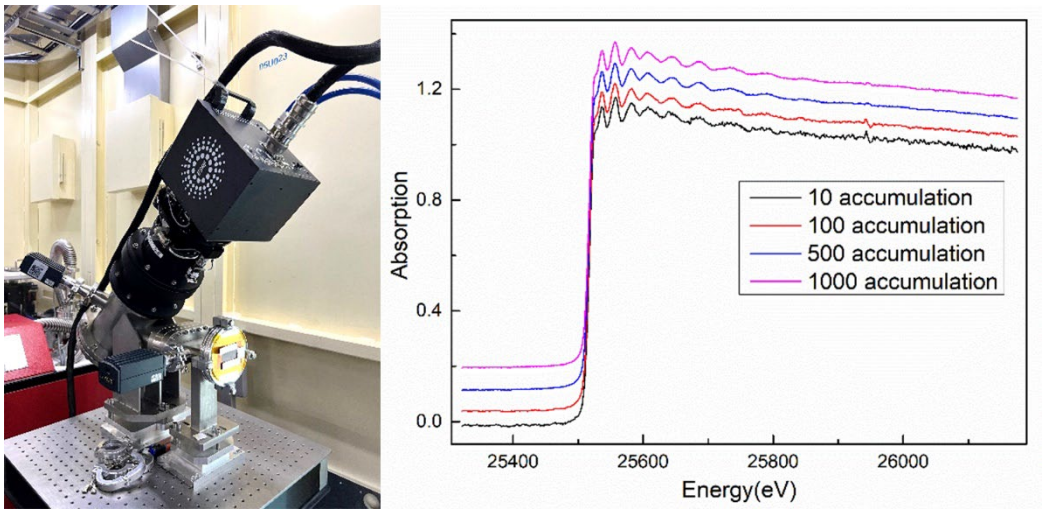

Fig. 10 Photograph (left) and sequence of Ag K-edge EXAFS (right) acquired using FReLoN 2D detector at D-Line.

3.2 Experimental methods

Compared with the normal energy-scanning XAFS, ED-XAS offers the following advantages: (1) Acquisition speed of microseconds—all energy points are acquired simultaneously by the PSD; (2) small focal spot size and high flux; and (3) high stability—no mechanical movement during acquisition.

3.2.1 Time-resolved ED-XAS

Rapid time resolution is an intrinsic feature of ED-XAS due to the parallel acquisition of an entire energy range. At D-Line, irreversible structural changes during the reactions or those stimulated via laser heating (~3000 K), pulse magnetic fields (30 T), and other in-situ equipment can be detected by rapid PSDs with a time resolution down to 2.5 μs. Fig. 11 shows the 1000 frame Cu K-edge XANES acquired at the D-Line under 40 kHz frame rate.

For the reversible ultrafast process, pump-probe ED-XAS can be used to detect the transient state structures, where the laser pulse “pump” the state from ground to excited, and then the delayed X-ray pulse, irradiating from the single electron bunch and with a length of approximately 100 ps, “probe” the transient structures during de-excitation. Pump-probe measurements must always be repeated tens of thousands of times to satisfy the requirements of spectral quality. The SSRF provides a hybrid mode to satisfy single bunch pump-probe experiments during ordinary user time.

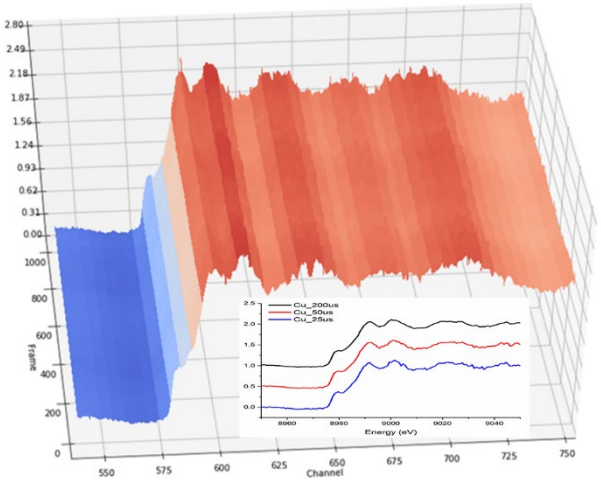

Fig. 11 1000 frames of Cu K-edge XANES with frame rate of 40 kHz.

3.2.2 Combined techniques of time-resolved ED-XAS+SR-IR

At D-Line, by deflecting the Infrared from the IR branch (BL06B) and transmitting it to the focus point of ED-XAS, the combined measurement of SR-IR and ED-XAS with rapid time resolution is realized using a dedicated in situ ED-XAS+IR coupling system. An IR servo system was installed before the IR spectrometer in the combination experimental station to ensure that the IR system can be adjusted at any time based on the X-ray focus position and that the parameters of the IR beam can satisfy the requirements of the experiment. To realize the coupling of the X-ray and IR beams at the sample point, a set of X-ray and IR coupling experimental systems that integrated IR focusing, spot-position adjustment, spot-position observation, and IR spectrum acquisition was developed. The IR spectral range of this system is 600–10000 cm^{-1}, the focusing spot size is approximately 25 μm@1000 cm^{-1}, and the coupling degree of two beams (X-ray and IR) is ~10 μm@1000 cm^{-1}.

Two sets of X-ray and IR coupling experimental equipment were developed at the D-Line: ED-XAS combined with transmission/reflection IR spectroscopy (Fig. 12), and ED-XAS combined with diffuse reflectance IR spectroscopy (DRIFTS) (Fig. 13). Based on a dedicated Schwarzschild focusing system, infrared and X-rays transmit through the sample in the same path, thus ED-XAS and transmitted IR measurements can be performed simultaneously at the same sample point. For this coupling experimental equipment, samples should have a certain IR transmission fraction. This system is based on a BrukerV80v FTIR instrument. The highest acquisition frequency is 400 kHz (2.5 μs/spectrum) for ED-XAS, whereas it is approximately 110 Hz at rapid scan mode (9 ms/spectrum, @16 cm^{-1} spectral resolution) for IR spectroscopy. The entire setup is mounted inside a Plexiglas box with N_2 flux to minimize the IR signals of H_2O and CO_2. The in-situ cell is positioned at the focal point of the IR light, and fine alignment is achieved using five-dimensional motorized motions. The maximum temperature achieved is 600 K. The windows are fabricated using CVD diamond, which not only allowed the transmission of IR and X-ray beams but also enabled the windows to withstand a certain reaction pressure.

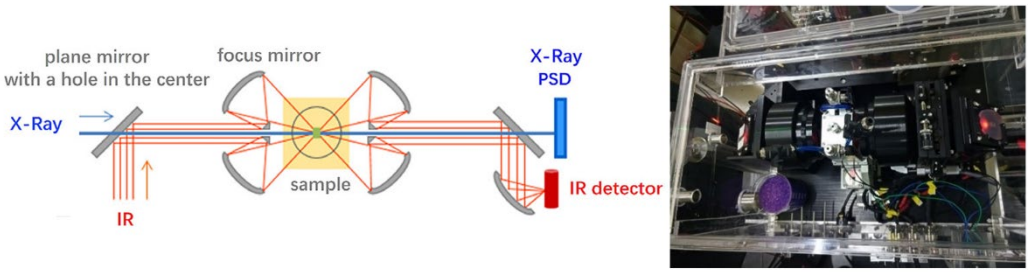

Fig. 12 Schematic illustration (left) and photograph (right) of ED-XAS+IR coupling system.

ED-XAS+DRIFTS was developed to investigate the samples under operating conditions such as catalysis in powder form during solid–gas reactions. The two spectra are acquired in-situ simultaneously at the near-surface layer of the sample. The cell is positioned at the focal spot of the diffuse spherical mirror, and fine alignment is achieved by the vertical movement of the entire cell and by the three motorized motions of the spherical mirror. Additionally, the spherical mirror serves as a gathering mirror for the diffuse reflection signals from the sample surface. In this configuration, X-rays are transmitted through the powder immediately below the sample surface, and the diffuse reflection IR originated from a sample volume of approximately tens of micrometers below the surface. The signals acquired using the two techniques are obtained from an almost identical sample volume. The small dead volume of the cell allows kinetic studies to be performed. The operating temperature is 300–873 K. The IR windows are fabricated using CaF_2, which is transparent in the mid-infrared region, whereas beryllium windows are selected for the X-ray beam, which allow the cell to withstand a pressure of approximately 1 bar. Meanwhile, five different thicknesses of the reactor (sample holder) are designed to adjust the sample thickness based on the requirement of ED-XAS measurement.

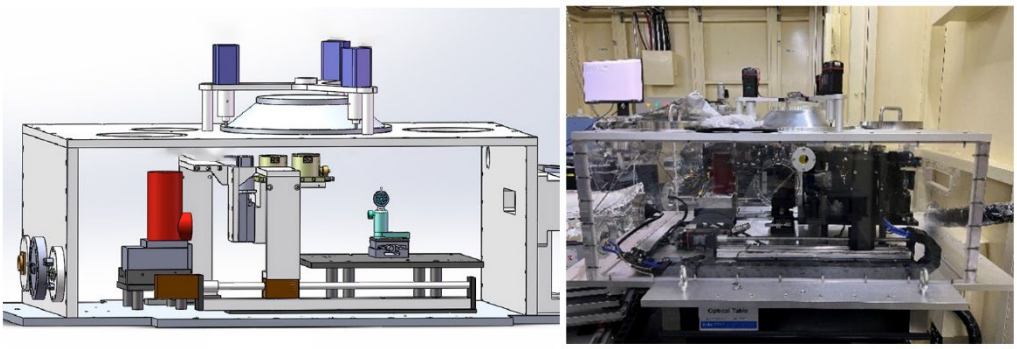

Fig. 13 Schematic illustration (left) and photograph (right) of ED-XAS+DRIFTS

coupling system.

3.2.3 Other methods

Owing to its intrinsic features of a small focus spot and high stability, ED-XAS is suitable for studies performed under extreme conditions, such as high temperature, high pressure, and strong pulsed magnetic fields [43,44]. At D-Line, ED-XAS is advantageous for high-pressure XAFS measurements involving a diamond anvil cell. Owing to the tapered undulator source in ED-XAS beamline, the flux at low energy is sufficiently high to overcome the strong absorption of the diamond anvils. Moreover, using the time structure of the electron bunch in the storage ring and a detector with a nanosecond electronic shutter, the time-resolution scale can be extended to the order of hundreds of picoseconds to perform ultrafast XAS, such as laser pump-X-ray probe experiments [45].

At D-Line, XMCD benefits from the stability of the abovementioned technique because the entire energy range of the spectrum is recorded in parallel [46-48]. The XMCD is the difference between the two X-ray absorption spectra obtained with right- and left-circularly polarized X-rays. In the hard X-ray regime, XMCD is bulk sensitive and can simultaneously provide information regarding the magnetic moment of the absorber atom as well as its local structural and electronic properties. Circularly polarized X-rays are generated by thin diamond (quarter-wave plates) placed between the polychromator and sample. Moreover, a 30 T pulsed magnetic field equipment with a cryogenically cooled solenoid coil was developed at the SSRF. Its main features are a pulse width of $\geqslant$ 0.66 ms and a repetition frequency of 0.02 Hz@30 T. The field repetition accuracy exceeded 0.5%. The sample temperatures can be changed from 3.5 K to 250 K in a He cryostat.

4. First commissioning results

The combination of SR-IR and ED-XAS allows one to simultaneously detect time-resolved atomic, electronic, and molecular structures. A mixture of KBr and DL-tyrosine was prepared. The thickness of this sample was calculated while ensuring certain transmission fractions for both IR light (@1591 cm^{-1}) and X-ray (@Br k-edge). At room temperature, the main absorption peak of DL-tyrosine is located at 1591 cm^{-1}, which corresponds to the N-H bending vibration of DL-tyrosine. At approximately

316 °C, DL- tyrosine will break down and the absorption peak at 1591 cm^{-1} will vanish. Based on the characteristics of the samples, the spectrum of Br K-edge EXAFS and the IR spectrum of DL-tyrosine are measured in transmission mode at room temperature (26 °C), 200 °C, and 330 °C. This coupling system was triggered by a synchronous clock control system. The IR and ED-XAS spectra acquired at different temperatures are shown in Fig. 14. The structure of KBr was extremely stable during the heating process. The structure of DL-tyrosine changed gradually with increasing temperature. At 330 °C, the absorption peak at 1591 cm^{-1} disappeared.

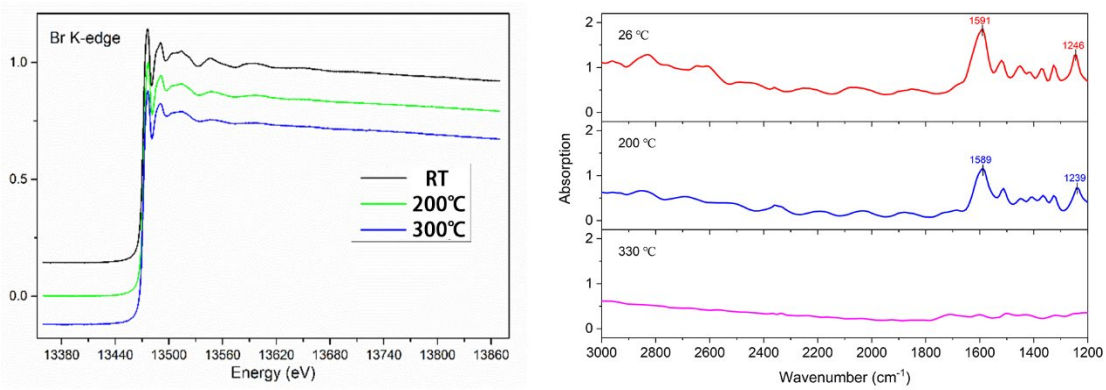

Fig. 14 Spectrum of Br K-edge EXAFS and IR spectrum of DL-tyrosine at different temperatures.

5. Summary and conclusion

The D-Line is the first beamline in the world to realize concurrent ED-XAS and SR-IR measurements at the same sample position. This combined method is effective for simultaneously investigating the atomic, electronic, and molecular structures of non-equilibrium processes in the fields of chemistry, physics, materials, and environmental science. Additionally, other distinctive techniques can be used on the beamline to achieve different scientific goals, such as time-resolved ED-XAS, high-pressure ED-XAS, XMCD, and pump–probe ED-XAS. With a time resolution of tens of microseconds, a focus spot of several micrometers, and high stability, D-Line enables many scientific issues to be investigated comprehensively.

6. Acknowledgements

We are grateful to the beamline engineers from the SSRF Optics and Control Department and the Mechanics and Vacuum Department for their effort on beamline design, construction, and online testing. We would like to thank the ESRF for their

technical support in providing us with the polychromator and 2D FReLoN detector. Additionally, we thank the PSI for its support in the manufacturing of the GOTTHARD II detector. We thank Sakura Pascarelli and Olivier Mathon from the ESRF, as well as François Baudelet and Qingyu Kong from SOLEIL for their fruitful discussions regarding energy-dispersive XAS techniques and beamline design. Finally, we thank Jiaguo Zhang from the PSI for his support with GOTTHARD detector installation and training.

References

1 H.J. Xu, Z.T. Zhao, Current status and progresses of SSRF project. Nucl. Sci. Tech. **19**, 1–6 (2008). doi:10.1016/S1001-8042(08)60013-5.
2 M.H. Jiang, X. Yang, H.J. Xu et al., Shanghai synchrotron radiation facility. Chin. Sci. Bull. **54**, 4171–4181 (2009). doi:10.1007/s11434-009-0689-y.
3 J.H. He, Z.T. Zhao, Shanghai synchrotron radiation facility. Natl. Sci. Rev. **1**, 171–172 (2014). doi:10.1093/nsr/nwt039.
4 H.S. Yu, X.J. Wei, J. Li, et al. The XAFS beamline of SSRF. Nucl. Sci. Tech. **26**, 050102 (2015). doi:10.13538/j.1001-8042/nst.26.050102.
5 W. Bras, G.E. Derbyshire, D. Bogg et al., Simultaneous studies of reaction kinetics and structure development in polymer processing. Science **267**, 996–999 (1995). doi:10.1126/science.267.5200.996.
6 P. Innocenzi, L. Malfatti, T. Kidchob et al., Time-resolved simultaneous detection of structural and chemical changes during self-assembly of mesostructured films. J. Phys. Chem. C **111**, 5345–5350 (2007). doi:10.1021/jp066566c.
7 A. Marcelli, D. Hampai, W. Xu et al., Time resolved IR and X-ray simultaneous spectroscopy: new opportunities for the analysis of fast chemical-physical phenomena in materials science. Acta Phys. Pol. A **115**, 489–500 (2009). doi:10.12693/APhysPolA.115.489.
8 A. Marcelli, P. Innocenzi, L. Malfatti et al., IR and X-ray time-resolved simultaneous experiments: an opportunity to investigate the dynamics of complex systems and non-equilibrium phenomena using third-generation synchrotron radiation sources. J. Synchrotron Radiat. **19**, 892–904 (2012). doi:10.1107/S0909049512041106.
9 M.A. Newton, Applying Dynamic and Synchronous DRIFTS/EXAFS to the Structural Reactive Behaviour of Dilute ($\leqslant$1wt%) Supported Rh/Al_2O_3 Catalysts using Quick and Energy Dispersive EXAFS. Top. Catal. **52**, 1410–1424 (2009). doi:10.1007/s11244-009-9321-2.
10 E. Becker, P.A. Carlsson, L. Kylhammar et al., *In situ* spectroscopic investigation of low-temperature oxidation of methane over alumina-supported platinum during periodic operation. J. Phys. Chem. C **115**, 944–951 (2011). doi:10.1021/jp103609n.
11 A. Iglesias-Juez, A. Kubacka, M. Fernández-García et al., Nanoparticulate Pd supported catalysts: size-dependent formation of Pd(I)/Pd(0) and their role in CO elimination. J. Am. Chem. Soc. **133**, 4484–4489 (2011). doi:10.1021/ja110320y.
12 T. Matsushita, R.P. Phizackerley, A fast X-ray absorption spectrometer for use with synchrotron radiation. Jpn. J. Appl. Phys. **20**, 2223 (1981). doi:10.1143/jjap.20.2223.
13 R.P. Phizackerley, Z.U. Rek, G.B. Stephenson et al., An energy-dispersive

spectrometer for the rapid measurement of X-ray absorption spectra using synchrotron radiation. J. Appl. Crystallogr. **16**, 220–232 (1983). doi:10.1107/S0021889883010286.

14 J. Headspith, G. Salvini, S.L. Thomas et al., XSTRIP—a silicon microstrip-based X-ray detector for ultra-fast X-ray spectroscopy studies. Nucl. Instrum. Meth. Phys. Res. Sect. A Accel. Spectrometers Detect. Assoc. Equip. **512**, 239–244 (2003). doi:10.1016/S0168-9002(03)01899-0.

15 I. Kantor, J.C. Labiche, E. Collet et al., A new detector for sub-millisecond EXAFS spectroscopy at the European Synchrotron Radiation Facility. J. Synchrotron Radiat. **21**, 1240–1246 (2014). doi:10.1107/S1600577514014805.

16 M. Borri, C. Cohen, J. Groves et al., Prototyping experience with Ge micro-strip sensors for EDXAS experiments. Nucl. Instrum. Meth. Phys. Res. Sect. A Accel. Spectrometers Detect. Assoc. Equip. **1017**, 165800 (2021). doi:10.1016/j.nima.2021.165800.

17 E. Dartyge, A.M. Flank, A. Fontaine et al., Synchrotron radiation plus photodiode array: exafs in dispersive mode for fast microanalysis. J. Phys. Colloques **45**, C2–275–C2–277 (1984). doi:10.1051/jphyscol:1984261.

18 H. Tolentino, E. Dartyge, A. Fontaine et al., X-ray absorption spectroscopy in the dispersive mode with synchrotron radiation: optical considerations. J. Appl. Crystallogr. **21**, 15–22 (1988). doi:10.1107/S0021889887008239.

19 A. Fontaine, F. Baudelet, E. Dartyge et al., Instrumentation and key elements of the dispersive X-ray absorption spectrometer for accurate measurements (invited) (abstract). Rev. Sci. Instrum. **66**, 1616 (1995). doi:10.1063/1.1145859.

20 F. Baudelet, Q. Kong, L. Nataf et al., ODE: a new beam line for high-pressure XAS and XMCD studies at SOLEIL. High Press. Res. **31**, 136–139 (2011). doi:10.1080/08957959.2010.532794.

21 F. Baudelet, E. Dartyge, A. Fontaine et al., Magnetic properties of neodynium atoms in Nd-Fe multilayers studied by magnetic X-ray dichroism on Nd LII and Fe K edges. Phys. Rev. B Condens. Matter **43**, 5857–5866 (1991). doi:10.1103/PhysRevB.43.5857.

22 O. Mathon, A. Beteva, J. Borrel et al., The time-resolved and extreme conditions XAS (TEXAS) facility at the European Synchrotron Radiation Facility: the general-purpose EXAFS bending-magnet beamline BM23. J. Synchrotron Radiat. **22**, 1548–1554 (2015). doi:10.1107/S160057751501783X.

23 G. Agostini, D. Meira, M. Monte et al., XAS/DRIFTS/MS spectroscopy for time-resolved operando investigations at high temperature. J. Synchrotron Radiat. **25**, 1745–1752 (2018). doi:10.1107/S160057751801305X.

24 M. Tada, Y. Uemura, R. Bal et al., *In situ* time-resolved DXAFS for the determination of kinetics of structural changes of H-ZSM-5-supported active re-cluster catalyst in the direct phenol synthesis from benzene and O2. Phys. Chem. Chem. Phys. **12**, 5701–5706 (2010). doi:10.1039/C000843P.

25 Y. Iwasawa, A. Suzuki, M. Nomura. Time-resolved energy-dispersive XAFS for in-situ characterization of nano-structures and catalysts. Phys. Scr. **115**, 59-65 (2005). doi:10.1238/Physica.Topical.115a00059.

26 K. Dohmae, Y. Nagai, T. Tanabe et al., Real-time XAFS analysis of Rh/alumina catalyst. Surf. Interface Anal. **40**, 1751–1754 (2008). doi:10.1002/sia.3003.

27 T. Fujimori, M. Takaoka, K. Kato et al., Observing copper chloride during dioxin formation using dispersive XAFS. X Ray Spectrom. **37**, 210–214 (2008). doi:10.1002/xrs.1038.
28 O. Sekizawa, T. Uruga, M. Tada et al., New XAFS beamline for structural and electronic dynamics of nanoparticle catalysts in fuel cells under operating conditions. J. Phys.: Conf. Ser. **430**, 012020 (2013). doi:10.1088/1742-6596/430/1/012020.
29 S. Diaz-Moreno, S. Hayama, M. Amboage et al., I20; the versatile X-ray absorption spectroscopy beamline at diamond light source. J. Phys.: Conf. Ser. **190**, 012038 (2009). doi:10.1088/1742-6596/190/1/012038.
30 Z. Jin, L. Wang, E. Zuidema et al., Hydrophobic zeolite modification for *in situ* peroxide formation in methane oxidation to methanol. Science **367**, 193–197 (2020). doi:10.1126/science.aaw1108.
31 X.P. Sun, F.F. Sun, S.Q. Gu et al., Local structural evolutions of $CuO/ZnO/Al_2O_3$ catalyst for methanol synthesis under operando conditions studied by *in situ* quick X-ray absorption spectroscopy. Nucl. Sci. Tech. **28**, 21 (2016). doi:10.1007/s41365-016-0170-y.
32 D.H. Deng, L. Yu, X.Q. Chen et al., Iron encapsulated within pod-like carbon nanotubes for oxygen reduction reaction. Angew. Chem. Int. Ed. **52**, 371–375 (2013). doi:10.1002/anie.201204958.
33 J.T. Hu, L. Yu, J. Deng et al., Sulfur vacancy-rich MoS_2 as a catalyst for the hydrogenation of CO_2 to methanol. Nat. Catal. **4**, 242–250 (2021). doi:10.1038/s41929-021-00584-3.
34 Y.F. Wu, L.L. Fan, Q.H. Liu et al., Decoupling the lattice distortion and charge doping effects on the phase transition behavior of VO_2 by titanium (Ti(4+)) doping. Sci. Rep. **5**, 9328 (2015). doi:10.1038/srep09328.
35 H.T. Wang, A. Ghosh, C.H. Wang et al., Evolution of superconductivity in $K_{2-x}Fe_{4+y}Se_5$: Spectroscopic studies of X-ray absorption and emission. Proc. Natl. Acad. Sci. **116**, 22458–22463 (2019). doi:10.1073/pnas.1912610116.
36 Z.H. Yu, M. Xu, Z.P. Yan et al., Pressure-induced isostructural phase transition and charge transfer in superconducting FeSe. J. Alloys Compd. **767**, 811–819 (2018). doi:10.1016/j.jallcom.2018.07.161.
37 B.G. Mao, T. Bao, J. Yu et al., One-pot synthesis of $MoSe_2$ hetero-dimensional hybrid self-assembled by nanodots and nanosheets for electrocatalytic hydrogen evolution and photothermal therapy. Nano Res. **10**, 2667–2682 (2017). doi:10.1007/s12274-017-1469-7.
38 L.Q. Wang, Y.X. Hao, L.M. Deng et al., Rapid complete reconfiguration induced actual active species for industrial hydrogen evolution reaction. Nat. Commun. **13**, 5785 (2022). doi:10.1038/s41467-022-33590-5.
39 J. Ye, C. Wang, C. Gao et al., Solar-driven methanogenesis with ultrahigh selectivity by turning down H_2 production at biotic-abiotic interface. Nat. Commun. **13**, 6612 (2022). doi:10.1038/s41467-022-34423-1.
40 W.X. Gou, M.G. Siebecker, Z.M. Wang et al., Competitive sorption of Ni and Zn at the aluminum oxide/water interface: an XAFS study. Geochem. Trans. **19**, 9 (2018). doi:10.1186/s12932-018-0054-7.
41 W.R. Cheng, H. Su, Q.H. Liu, Tracking the oxygen dynamics of solid–liquid

electrochemical interfaces by correlative *in situ* synchrotron spectroscopies. Acc. Chem. Res. **55**, 1949–1959 (2022). doi:10.1021/acs.accounts.2c00239.

42 A. San-Miguel, M. Hagelstein, J. Borrel et al., An exchangeable Bragg/Laue polychromator for energy-dispersive XAFS. J. Synchrotron Radiat. **5**, 1396–1397 (1998). doi:10.1107/S0909049598011315.

43 J.P. Itie, A. Polian, G. Calas et al., Pressure-induced coordination changes in crystalline and vitreous GeO_2. Phys. Rev. Lett. **63**, 398–401 (1989). doi:10.1103/PhysRevLett.63.398.

44 A.V. Sapelkin, S.C. Bayliss, A.G. Lyapin et al., Structural studies of bulk amorphous GaSb under high pressures. Phys. Status Solidi B. **198**, 503–508 (1996). doi:10.1002/pssb.2221980166.

45 J. He, M. Liu, C.X. Yin et al., Experimental studies on the X-ray single-pulse jitter at the SSRF. Nucl. Instrum. Meth. Phys. Res. Sect. A Accel. Spectrometers Detect. Assoc. Equip. **1025**, 166038 (2022). doi:10.1016/j.nima.2021.166038.

46 F. Baudelet, S. Odin, C. Giorgetti et al., ptFe_3Invar studied by high pressure magnetic circular dichroism. J. Phys. IV France **7**, C2–441–C2–442 (1997). doi:10.1051/jp4/1997042.

47 C. Giles, C. Malgrange, J. Goulon et al., Energy-dispersive phase plate for magnetic circular dichroism experiments in the X-ray range. J. Appl. Crystallogr. **27**, 232–240 (1994). doi:10.1107/S0021889893007976.

48 O. Mathon, F. Baudelet, J.P. Itié et al., XMCD under pressure at the Fe K edge on the energy-dispersive beamline of the ESRF. J. Synchrotron Radiat. **11**, 423–427 (2004). doi:10.1107/S0909049504018862.